increase the computational time; therefore, they are applicable for large-scale engineering calculations.

Acknowledgment

This work was partially supported by FFA, the Aeronautical Research Institute of Sweden.

References

[1]Baldwin, B. S., and Lomax, H., "Thin Layer Approximation and Algebraic Model for Separated Turbulent Flow," AIAA Paper 78-257, Jan. 1978.

[2]Chien, K. Y., "Predictions of Channel and Boundary Layer Flows with a Low Reynolds Number Turbulence Model," *AIAA Journal*, Vol. 20, No. 1, 1982, pp. 33–38.

[3]Baysal, O., and Hoffman, W. B., "Simulation of Three-Dimensional Shear Flow Around a Nozzle-Afterbody at High Speeds," *Journal of Fluids Engineering*, Vol. 114, June 1992, pp. 178–185.

[4]Launder, B. E., and Priddin, C. H., "A Comparison of Some Proposals for the Mixing Length Near a Wall," *International Journal of Heat and Mass Transfer*, Vol. 16, No. 3, 1973, pp. 700–702.

[5]Nichols, R. H., "A Two-Equation Model for Compressible Flows," AIAA Paper 90-0494, Jan. 1990.

[6]Hu, J., and Rizzi, A., "Assessment of Compressibility and Pressure-Gradient Corrections for Modeling Turbulent Hypersonic Nozzle Flows," AIAA Paper 95-2313, June 1995.

[7]Rizzi, A., Eliasson, P., Lindblad, I., Hirsch, Ch., Lacor, C., and Haeuser, J., "The Engineering of Multiblock/Multigrid Software for Navier–Stokes Flows on Structured Meshes," *Computers and Fluids*, Vol. 22, No. 2/3, 1993, pp. 341–367.

[8]Hovstadius, G., "Measurement of Boundary Layer Properties in Two Hypersonic Nozzles," Aeronautical Research Inst. of Sweden, FFA Rept. AU-624, Stockholm, Sweden, May 1971.

K. J. Weilmuenster
Associate Editor

Dual-Code Solution Strategy for Hypersonic Flows

William A. Wood* and Richard A. Thompson*
NASA Langley Research Center, Hampton, Virginia 23681-0001
and
Scott Eberhardt†
University of Washington, Seattle, Washington 98195

Nomenclature

C_p	= frozen specific heat at constant pressure, J/kg-K
c	= mass fraction
E_t	= volume-specific total energy, J/m^3
e	= internal energy, (m/s)^2
H	= mixture enthalpy, (m/s)^2
h	= enthalpy, (m/s)^2
h_0	= reference enthalpy at the reference temperature, (m/s)^2
M	= Mach number
$\bar{M}$	= molecular weight, kg/kg-mole
P	= pressure, Pa
q	= heat-transfer rate, W/m^2
R_n	= nose radius, m
$\bar{R}$	= universal gas constant, 8314.3 J/kg-mole-K
T	= temperature, K
u, v, w	= Cartesian velocity components, m/s
X	= axial coordinate, m
α	= angle of attack, deg
ρ	= density, kg/m^3

Subscripts

l	= LAURA
s	= species
u	= UPS
∞	= freestream value

Received June 20, 1995; revision received Nov. 15, 1995; accepted for publication Dec. 11, 1995.

*Aerospace Technologist, Aerothermodynamics Branch, Gas Dynamics Division. Member AIAA.

†Associate Professor, Department of Aeronautics and Astronautics. Member AIAA.

Introduction

INTEREST in reducing the cost of access to space[1] has led to many proposals for advanced launch vehicles that are either fully or partially reusable. Most of these configurations, e.g., the follow-on to Orbital Science's Pegasus[2] and NASA's Single-Stage Vehicle,[1] incorporate slender, blunted configurations. The design process for these vehicles will heavily rely on computational methods to define the aerothermodynamic environment during re-entry.

A popular and proven code developed to solve the re-entry environment is the Navier–Stokes solver Langley Aerothermodynamic Upwind Relaxation Algorithm (LAURA).[3] LAURA is a finite volume, shock-capturing algorithm with second-order spatial accuracy for the steady-state solution of viscous or inviscid hypersonic flows. The scheme employs a point implicit relaxation strategy with upwind-biased flux-difference splitting for perfect gas, equilibrium air, or nonequilibrium air calculations. Although LAURA has successfully computed viscous, reacting flowfields about the Shuttle Orbiter configuration,[4] the time-relaxation approach to solve the thin-layer Navier–Stokes (TLNS) equations can require excessive computational time and memory resources. Several solution strategies have recently been attempted to reduce these computational requirements of a full-vehicle LAURA solution.

Weilmuenster and Gnoffo[5] proposed a multiblock solution procedure, in which the domain is divided into blocks ordered in the streamwise direction. This procedure principally attacks the memory requirements inherent in obtaining a full-body TLNS solution by splitting the domain, but does not decrease the time required to obtain the solution since the TLNS equations remain the governing equations. Greene[6] has extended the LAURA code into a parabolized Navier–Stokes (PNS) version, but this particular formulation, being a TLNS extension, is locally iterative in pseudotime steps, and its performance suffers from arriving as a PNS solver via a TLNS algorithm, rather than being a code that was optimized as a PNS solver from inception. Thus, although this method significantly reduced the memory required to obtain a solution, it was not able to reduce solution time to the level desired.

Upwind parabolized Navier–Stokes Solver (UPS)[7] was identified as a code that, when combined with LAURA, might provide the tremendous reduction in vehicle solution time originally sought with the LAURA–TLNS/LAURA–PNS method. UPS is an upwind, finite volume, state-of-the-art PNS code with perfect gas, equilibrium air, and chemical nonequilibrium capability. It is second-order accurate in the crossflow plane and first-order accurate in the marching direction.

UPS has been used in conjunction with the TLNS code compressible Navier–Stokes solver by Lawrence et al.[8] for perfect gas computations. Nonequilibrium air solutions started from an axisymmetric TLNS code TUFF are presented in Refs. 9–11.

The present study looks to combine two well-established computational codes, LAURA and UPS, for the consistent solution of perfect gas, equilibrium,[12] and chemically reacting hypersonic flowfields. Significantly faster and less costly vehicle aerothermodynamics are sought without compromising the accuracy and sophistication of a full-body LAURA solution. The technique is demonstrated on a blunted, multiconic geometry at angle of attack.

Present Method

The present method seeks to reduce both the computational time and memory associated with obtaining a full-body LAURA solution

for large re-entry vehicles. The procedure uses LAURA to obtain the flowfield definition in the blunted nose region, extracts the necessary starting data and manipulates it for compatibility, and then marches UPS down the slender vehicle afterbody. Any inviscid subsonic flow regions must be completely encompassed within the LAURA portion of the solution to avoid violation of the PNS assumptions.

From the converged LAURA nose solution a crossflow plane of data is extracted to initialize the UPS marching solution. Currently, this plane is chosen at least three cells upstream of the LAURA domain outflow plane to avoid any possible contamination from the extrapolated outflow boundary conditions.

Since both LAURA and UPS are structured finite volume formulations, the UPS starting plane grid can be extracted directly from the LAURA volume grid. Coordinate rotation transformations are required for both physical and curvilinear coordinate systems.

The standard LAURA restart file contains three flow velocity components, temperature, and species densities. A UPS restart requires mixture density, three momentum components, specific total energy, mixture molecular weight, and species mass fractions.

The total density is found from summing the species densities:

$$\rho_u = \sum_s \rho_{s_l} \tag{1}$$

and the species mass fractions follow as

$$c_{s,u} = \rho_{s_l}/\rho_u \tag{2}$$

The three components of momentum are obtained directly from the velocity components and the total density, with coordinate rotations as

$$\rho u_u = \rho_u \times (-w_l), \qquad \rho v_u = \rho_u \times u_l, \qquad \rho w_u = \rho_u \times v_l \tag{3}$$

The mixture molecular weight is found from the equation of state:

$$\bar{M}_u = \rho_u \bar{R} T_l / P_u \tag{4}$$

where the mixture pressure was determined from summing the species partial pressures,

$$P_u = \rho_u \sum_s \left(\frac{c_{s_u} \bar{R} T_l}{\bar{M}_s} \right) \tag{5}$$

a step consistent with the assumption, common to both codes, that the working fluid is a mixture of ideal gases.

The volume-specific total energy is determined from the temperature and species concentrations as

$$E_{t_u} = \rho_u \left[\tfrac{1}{2} \left(u_l^2 + v_l^2 + w_l^2 \right) + e_u \right] \tag{6}$$

where

$$e_u = H_u - P_u/\rho_u \tag{7}$$

$$H_u = \sum_s h_{s_u} c_{s_u} \tag{8}$$

$$h_{s_u} = C_{p,s_u} T_l + h_{0,s_u} \tag{9}$$

Energies were calculated using both the UPS enthalpy tables and the LAURA enthalpy curve fits. For some cases, however, the PNS solution developed instabilities at the wall when the LAURA enthalpy curve fits were employed, and so the interface calculation in Eq. (9) uses the UPS values for the specific heat and reference enthalpy.

Grid adaptions are performed during the LAURA solution to align the grid with the bow shock and set the wall grid spacing to a specified nominal cell Reynolds number, based on the local speed of sound. This spacing is retained in the extrapolation to the UPS grid, while the outer points are smoothly distributed to capture the downstream shock. This procedure is not currently fully integrated with the UPS solution in the present method and relies on user-specified stretching parameters.

Of the five kinetic models available in LAURA, the model of Kang et al.[13] was chosen as being the closest match with the Blottner[14] rates used in UPS. There are differences in the transport computations between the two codes, which for some cases have been seen to lead to differences in thermal conductivity at typical wall conditions of 5%.

Results

Mach-28, seven-species, single-temperature flow of air over the sphere–cone–cylinder–flare configuration studied by Bhutta et al.[15] is computed at 5-deg angle of attack. This configuration has a 0.1524-m spherical nosecap followed by a 9-deg cone. After 10 nose radii, the cone is followed by a cylinder and then a 5-deg flare, each of 10-nose-radii length. The freestream conditions correspond to an altitude of 83.8 km at a Reynolds number per meter of 6.148×10^3. A fully catalytic wall boundary condition is employed, setting the wall species concentrations equal to their freestream values. Freestream mass fractions of nitrogen and oxygen are 0.767 and 0.233, respectively. A fixed wall temperature of 833 K is used.

Both a full-vehicle LAURA solution and combined LAURA–UPS solution were obtained for this case. The full LAURA grid contains 51 streamwise cells, 18 circumferential cells, and 128 radial cells. Grid convergence for this case is assessed in Ref. 16. The UPS starting plane was extracted from the LAURA solution at 2 nose radii, and marched with a 0.01-m step size.

Figure 1 plots both windside and leeside centerline heat transfer rates from the full-body LAURA and LAURA–UPS solutions along with the PNS solution from Ref. 15. Leeside agreement is excellent between all three solutions, with the present method matching the full-body LAURA solution to within 3%. The windside agreement is fair, though not as good as the leeside. On the windside centerline the UPS heating is 10% higher on the cone, 7% higher on the cylinder, and 18% higher on the flare. Also, the UPS and LAURA heating trends appear to separate at the tail end of the body.

The windside and leeside surface pressures from the full-body LAURA and combined LAURA–UPS solutions are shown in Fig. 2. For the surface pressure, good agreement is seen on the windside, with a maximum 8% difference in results. The leeside agreement is good on the cone and flare, but not good on the cylindrical midsection, where a 12% difference is seen. In this region of the leeside midsection the PNS equations may be expected to be more accurate than the TLNS equations, which neglect crossflow viscous terms.

The CPU time required for convergence of the full-body LAURA solution was 20 h on a Cray Y-MP. With the combined procedure the LAURA nose solution took 1.3 h and the UPS portion took just 0.2 h, for a total time of 1.5 h, a 92% reduction over the full-body LAURA solution time. The full LAURA solution used 25 MW of memory, whereas the combined LAURA–UPS solution required 8 MW of memory for the nose solution and 2.2 MW for the UPS afterbody solution.

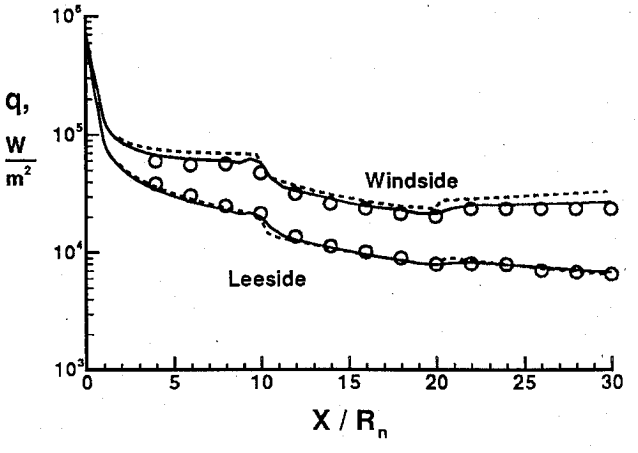

Fig. 1 Symmetry-plane heat-transfer rates: $M = 28$, $R_n = 0.1524$ m, fully catalytic wall, $\alpha = 5$ deg; ——, LAURA; - - - -, LAURA–UPS; and ○, PNSNQ3D.

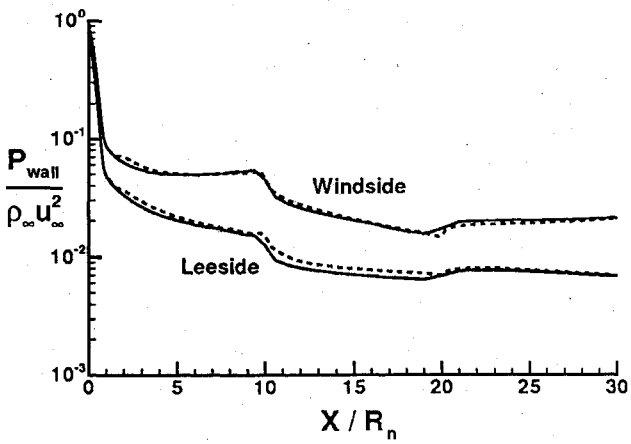

Fig. 2 Symmetry-plane surface pressures: $M = 28$, $R_n = 0.1524$ m, fully catalytic wall, $\alpha = 5$ deg; ——, LAURA and - - - -, LAURA–UPS.

Concluding Remarks

Two proven, existing solvers have been combined for the aerothermodynamic solution of hypersonic air flowfields with finite-rate chemistry. The robustness of the TLNS solver LAURA has been joined with the speed of the PNS solver UPS. The class of vehicles to which the method is applicable are blunt-nosed configurations with afterbody flowfields free of streamwise-separated flow. The method offers the potential benefits of obtaining efficient solutions with second-order accuracy in the crossflow planes, while requiring only a fraction of the computer time and memory that a full-body LAURA solution would require.

References

[1]Bekey, I., Powell, R., and Austin, R., "NASA Studies Access to Space," *Aerospace America*, Vol. 32, No. 3, 1994, pp. 38–43.

[2]Foley, T. M., "Big Hopes for Small Launchers," *Aerospace America*, Vol. 33, No. 7, 1995, pp. 28–34.

[3]Gnoffo, P. A., Gupta, R. N., and Shinn, J. L., "Conservation Equations and Physical Models for Hypersonic Air Flows in Thermal and Chemical Nonequilibrium," NASA TP 2867, Feb. 1989.

[4]Kleb, W. L., and Weilmuenster, K. J., "Characteristics of the Shuttle Orbiter Leeside Flow During a Reentry Condition," AIAA Paper 92-2951, July 1992.

[5]Weilmuenster, K. J., and Gnoffo, P. A., "Solution Strategies and Heat Transfer Calculations for Three-Dimensional Configurations at Hypersonic Speeds," AIAA Paper 92-2921, July 1992.

[6]Greene, F. A., "An Upwind-Biased Space Marching Algorithm for Supersonic Viscous Flow," NASA TP 3068, March 1991.

[7]Buelow, P. E., Tannehill, J. C., Ievalts, J. O., and Lawrence, S. L., "Three-Dimensional, Upwind, Parabolized Navier–Stokes Code for Chemically Reacting Flows," *Journal of Thermophysics and Heat Transfer*, Vol. 5, No. 3, 1991, pp. 274–283.

[8]Lawrence, S. L., Kaul, U., and Tannehill, J. C., "UPS Code Enhancements," Sixth National Aerospace Plane Technology Symposium, Paper 16, April 1989.

[9]Buelow, P., Ievalts, J., and Tannehill, J., "Comparison of Three-Dimensional Nonequilibrium PNS Codes," AIAA Paper 90-1572, June 1990.

[10]Lawrence, S., "Application of Space-Marching Methods to Hypersonic Forebody Flow Fields," AIAA Paper 92-5030, Dec. 1992.

[11]Muramoto, K. K., "The Prediction of Viscous Nonequilibrium Hypersonic Flows About Ablating Configurations Using an Upwind Parabolized Navier–Stokes Code," AIAA Paper 93-2998, July 1993.

[12]Wood, W. A., and Thompson, R. A., "Combined LAURA-UPS Hypersonic Solution Procedure," NASA TM 107682, March 1993.

[13]Kang, S.-W., Dunn, M. G., and Jones, W. L., "Theoretical and Measured Electron-Density Distributions for the RAM Vehicle at High Altitudes," AIAA Paper 72-689, June 1972.

[14]Blottner, F. G., Johnson, M., and Ellis, M., "Chemically Reacting Viscous Flow Program for Multicomponent Gas Mixtures," Sandia National Labs., SC-RR 70-754, Albuquerque, NM, Dec. 1971.

[15]Bhutta, B. A., Lewis, C. H., and Kautz, F. A., "A Fast Fully-Iterative Parabolized Navier–Stokes Scheme for Chemically-Reacting Reentry Flows," AIAA Paper 85-0926, June 1985.

[16]Wood, W. A., "Dual-Code Solution Strategy for Chemically-Reacting Hypersonic Flows," AIAA Paper 95-0158, Jan. 1995.

T. C. Lin
Associate Editor

Reevaluation of Flight-Derived Surface Recombination-Rate Expressions for Oxygen and Nitrogen

R. N. Gupta*
NASA Langley Research Center, Hampton, Virginia 23681-0001

Introduction

FOR the efficient design of future transportation systems, an accurate description of the re-entry aerothermal environment about a spacecraft is important. Since the maximum heating pulse for such a lifting body is likely to occur at high altitudes, surface recombination rates for the dissociated air species (in a flowfield with nonequilibrium chemistry) are required in the evaluation of spacecraft heating. Unfortunately, direct measurement of surface recombination rates (on surface coatings) is not possible from ground or flight tests. These rates are generally inferred from the surface heat-flux measurements.

In the study of Ref. 1, an expression for oxygen recombination coefficient was obtained for the Space Shuttle tile material based on the heat-flux measurements (obtained from the early Shuttle flight test missions). Unfortunately, some discrepancies in the version of the viscous shock-layer (VSL) code[2] used in Ref. 1 were discovered during the studies of Refs. 3–5. The present investigation accounts for those discrepancies in the reevaluation of surface recombination-rate expressions for oxygen and nitrogen from the flight data.

Analysis

Procedures used to develop the present expressions for the surface reaction-rate coefficients are the same as those employed in Ref. 1. The surface recombination-rate values that give the best fit to flight heating rates at STS-2 entry conditions for altitudes of 71.29, 74.98, and 77.91 km are correlated as a function of the surface temperature in an Arrhenius form. The reaction-rate values are incorporated in a detailed VSL code[3,4] for the finite reacting flowfields to compute laminar heating rates for the partially catalytic surfaces. A brief outline of the procedure, as well as the relative merits of the flowfield method for computing the flow in the Shuttle windward symmetry plane, is given in Ref. 1. Only the changes implemented in the code employed for the study of Ref. 1 are provided here.

First, the shock boundary condition for enthalpy is correctly specified[5] and referenced to a temperature of 298 K. Next, a coding error in implementation of the constant Prandtl number option in the code[6] used in Refs. 1 and 2 has been rectified. Also, new transport and thermodynamic properties[7] are employed in place of those from Refs. 8 and 9. Finally, a grid-independent solution is obtained by employing a stepsize ΔS of 0.1 in the streamwise direction for the entire Shuttle length and a variable stepsize $\Delta\eta$ (with a value of 1×10^{-4} at the surface) in the direction normal to the surface. References 1 and 2 used similar values of $\Delta\eta$; however, ΔS varied from 0.1 in the stagnation region increasing through the nose region to a value of 3.0 at the tail end of Shuttle. Although the influence of each change on the predicted values of Ref. 1 is not quantified here, the effect of ensuring axial grid independence, in general, was the largest in developing the correlations. This is because the surface distributions of pressure and heating vary considerably in the nose

Received Oct. 5, 1995; revision received Nov. 24, 1995; accepted for publication Dec. 14, 1995.

*Senior Research Engineer, Aerothermodynamics Branch, Gas Dynamics Division. Associate Fellow AIAA.